Numerical Determination of Hysteresis Parameters for the Modeling of Magnetic Properties Using the Theory of Ferromagnetic Hysteresis

David C. Jiles, *Senior Member, IEEE,* J. B. Thoelke, and M. K. Devine

Abstract—**This paper describes how the various model parameters needed to describe hysteresis on the basis of the Jiles-Atherton theory can be calculated from experimental measurements of the coercivity, remanence, saturation magnetization, initial anhysteretic susceptibility, initial normal susceptibility, and the maximum differential susceptibility. The determination of hysteresis parameters based on this limited set of magnetic properties is of the most practical use since these are the properties of magnetic materials that are most likely to be available.**

Introduction

In previous papers, the problem of modeling ferromagnetic hysteresis has been discussed [1], [2], and from a consideration of the underlying mechanism of domain wall motion, two differential equations have been derived which represent the irreversible differential susceptibility and the reversible differential susceptibility [3]. The solution of these differential equations, when combined with an appropriate choice of function for the anhysteretic magnetization, leads to a normal sigmoid-shaped hysteresis curve. This paper derives the equations in the inversion algorithm which are used for determining the model parameters from experimental data.

Equation of Hysteresis

The previous development of the equations is first summarized with k redefined in units of $A \cdot m^{-1}$ instead of tesla. This leads to a more useful result because for very soft magnetic materials, k then becomes equal to the coercivity H_c, which is measured in $A \cdot m^{-1}$.

Irreversible Differential Susceptibility

The energy lost to pinning is expressed as a function of the irreversible change in magnetization M_{irr} [3] by the equation

$$E_{pin}(M_{irr}) = \frac{n\langle \epsilon_\pi \rangle}{2m} \int_0^{M_{irr}} dM_{irr} \tag{1}$$

where n is the number density of pinning sites, $\langle \epsilon_\pi \rangle$ is the average pinning energy of the sites for 180° domain walls, and m is the magnetic moment of a typical domain. If the coefficient $n\langle \epsilon_\pi \rangle / 2m$ on the right-hand side is expressed in terms of a single parameter k by the equation

$$\mu_0 k = \frac{n\langle \epsilon_\pi \rangle}{2m}, \tag{2}$$

this leads to

$$E_{pin}(M_{irr}) = \mu_0 k \int_0^{M_{irr}} dM_{irr} \tag{3}$$

where k is now in units of $A \cdot m^{-1}$. The hysteresis equation for irreversible changes in magnetization can be derived from (3), and this can be shown to be [3]

$$M_{irr} = M_{an} - k\delta \frac{dM_{irr}}{dH_e} \tag{4}$$

where H_e is the effective field, defined as

$$H_e = H + \alpha M \tag{5}$$

and δ is a directional parameter having the value $+1$ for $dH/dt > 0$ and -1 for $dH/dt < 0$. Equation (4) above may be rearranged, providing $k \neq 0$ and $k\delta - \alpha(M_{an} - M_{irr}) \neq 0$, to give the equation for the differential irreversible susceptibility:

$$\frac{dM_{irr}}{dH} = \frac{M_{an} - M_{irr}}{k\delta - \alpha(M_{an} - M_{irr})}. \tag{6}$$

Reversible Differential Susceptibility

The component of reversible magnetization reduces the difference between the prevailing irreversible magnetization M_{irr} and the anhysteretic magnetization M_{an} at the given field strength. This can be expressed as

$$M_{rev} = c(M_{an} - M_{irr}) \tag{7}$$

since the amount of bending of the domain walls is dependent on the difference between the anhysteretic magnetization and the irreversible magnetization M_{irr} [3]. Consequently,

$$\frac{dM_{rev}}{dH} = c\left(\frac{dM_{an}}{dH} - \frac{dM_{irr}}{dH}\right). \tag{8}$$

Manuscript received November 19, 1990; revised August 28, 1991. This work was performed for the U.S. Department of Energy by Iowa State University under Contract W-7405-ENG-82.

The authors are with the Ames Laboratory, Iowa State University, Ames, IA 50011.

IEEE Log Number 9104973.

0018-9464/92$03.00 © 1992 IEEE

Total Differential Susceptibility

Summation of the reversible and irreversible components of the differential susceptibility leads to the total differential susceptibility dM/dH:

$$\frac{dM}{dH} = (1 - c) \frac{M_{an} - M_{irr}}{k\delta - \alpha(M_{an} - M_{irr})} + c \frac{dM_{an}}{dH}. \quad (9)$$

The exact form of this equation is slightly different from that used in the earlier paper [3] because of the altered forms of (6) and (7) which allow complete separation of the reversible and irreversible contributions to the differential susceptibility at any point on the hysteresis curve. (Ultimately, this only has the effect of changing the value of c, the form of the hysteresis curves remaining identical.)

Solutions of the Hysteresis Equations

It has been found most convenient from the viewpoint of numerical solutions for hysteresis modeling to first solve (6) for the irreversible component of magnetization and then add the reversible component by solving (7). It should be noted that some unphysical solutions to (6) can be obtained when the magnetic field is reduced from the extremity of the loop (i.e., the loop tip) when the magnetization M_{irr} is below the anhysteretic M_{an} in the first quadrant or above the anhysteretic in the third quadrant. In this case, direct solution of (6) leads to a negative differential susceptibility as the field is reduced. In fact, under these conditions, the domain walls actually remain pinned on the defect sites, and so $dM_{irr}/dH = 0$. However, at this stage, the reversible changes in magnetization are still operative, so that a bulged domain wall will relax as the field is reduced. This means that as the field is reduced from the loop tip, until the magnetization crosses the anhysteretic, the change in magnetization is almost reversible, and therefore on the basis of the model, $dM/dH \simeq dM_{rev}/dH$ in this region.

Example Solutions of the Model Equations

Some example solutions of the model equations of hysteresis are shown in Figs. 1, 2, 3, and 4 for various values of the hysteresis parameters. These results give some indication of the range of hysteresis loops which can be obtained from solving the hysteresis equations. It can be seen that the model is not just restricted to soft magnetic materials, but also can be used for hard magnetic materials. For example, in Fig. 4, the coercivity is 0.41×10^6 A/m (5.125 kOe).

Parameter Extraction from Experimental Data

Until now, it has not been clear how to calculate the model parameters a, α, k, and c from a set of experimental data in the form of a hysteresis loop. This is a difficult procedure since it is not immediately clear which "fixed reference points" on a measured hysteresis curve should be used to calculate the parameters. Furthermore, the implicit nature of the hysteresis equations makes the problem intractable for an injudicious choice of these fixed points. It has been found that the simplest solution to the problem is obtained by using the initial normal susceptibility χ'_{in}, the initial anhysteretic susceptibility χ'_{an}, the coercivity H_c, the differential susceptibility at the coercive point χ'_{H_c}, the remanence M_r, the differential susceptibility at remanence χ'_{M_r}, and the coordinates H_m, M_m of a loop tip, together with the differential susceptibility of the initial magnetization curve at the loop tip χ'_m. From these measured magnetic properties, the parameters governing the hysteresis equations can be calculated. In many cases, this calculation will be sufficient for modeling purposes; in other cases, it can be used as a first approximation forming a basis for subsequent refinement.

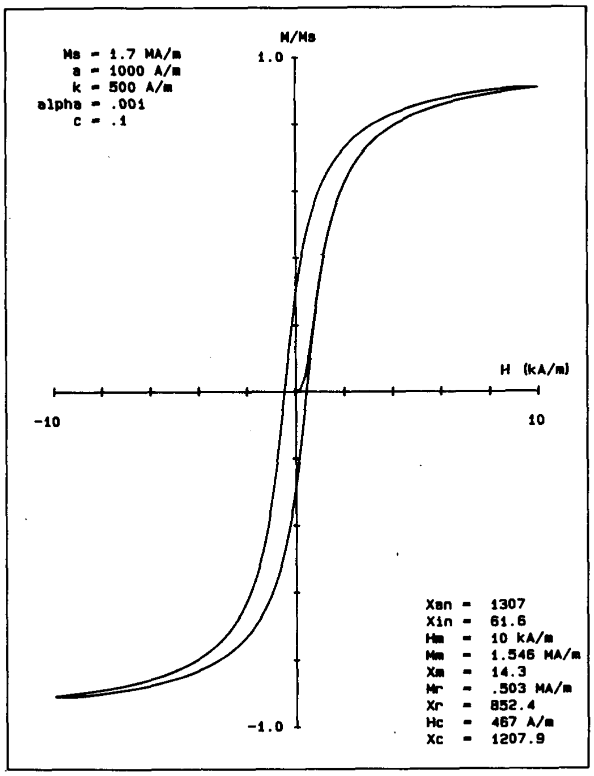

Fig. 1. Theoretical hysteresis loop obtained from solution of the model equations with $M_s = 1.7 \times 10^6$ A · m^{-1}, $a = 1000$ A · m^{-1}, $k = 500$ A · m^{-1}, $\alpha = 0.001$, $c = 0.1$.

Saturation Magnetization M_s

The easiest parameter to obtain is the saturation magnetization M_s. This is often known for a particular material, and so can be obtained from data sheets or other references. It can also be measured as closely as desired by subjecting the material to a field of arbitrarily high strength, and then either measuring the flux density B with a coil or the magnetization M with a vibrating sample magnetometer, and then calculating M_s from these measurements.

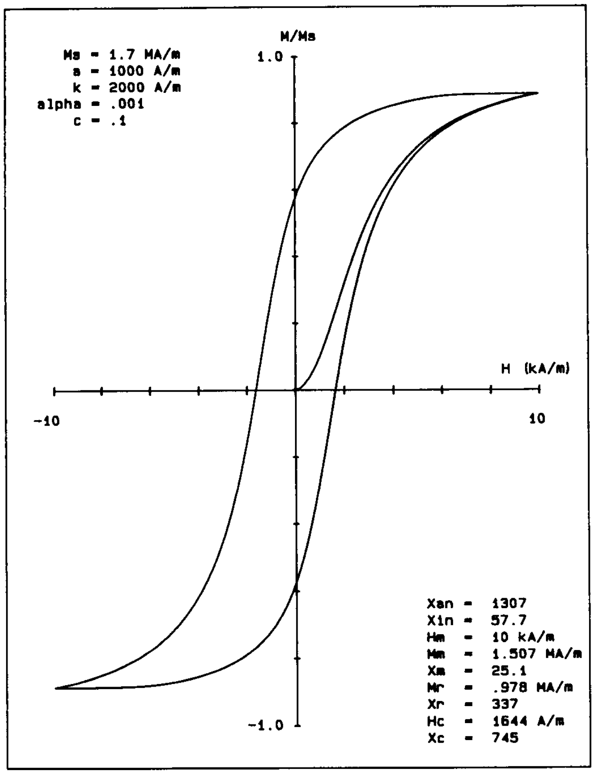

Fig. 2. Theoretical hysteresis loop obtained from solution of the model equations with $M_s = 1.7 \times 10^6$ A · m^{-1}, $a = 1000$ A · m^{-1}, $k = 2000$ A · m^{-1}, $\alpha = 0.001$, $c = 0.1$.

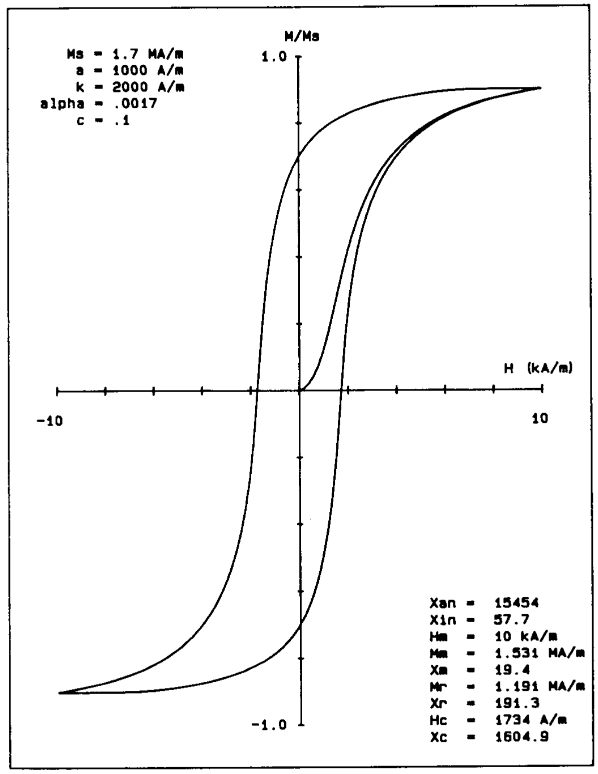

Fig. 3. Theoretical hysteresis loop obtained from solution of the model equations with $M_s = 1.7 \times 10^6$ A · m^{-1}, $a = 1000$ A · m^{-1}, $k = 2000$ A · m^{-1}, $\alpha = 0.0017$, $c = 0.1$.

Determination of the Parameter c which Represents Reversible Wall Motion

The reversible component of magnetization due to reversible wall bending and reversible translation is determined in the model by the coefficient c. This can be calculated from the ratio of the initial normal susceptibility $\chi'_{in} = (dM/dH)_{H=0, M=0}$ to the initial anhysteretic susceptibility $\chi'_{an} = (dM_{an}/dH)_{H=0, M=0}$. The actual relationship depends on the method of numerical solution used because the equations are implicit in M, and although $c \approx (3a - \alpha M_s/M_s)\chi'_{in}$, the method which is used here assumes that the anhysteretic M_{an} which is effective at any given point on the M, H plane depends only on the prevailing values of M and H.

From (9) above, consider the situation at the origin of the initial magnetization curve. Here, $M_{irr} = 0$, and since at the very origin the small incremental magnetization changes must be totally reversible, we have $dM_{irr}/dH = 0$. Therefore, from (9), we arrive at

$$\chi'_{in} = \left(\frac{dM}{dH}\right)_{\substack{H=0\\M=0}} = \frac{(1-c)M_{an}}{k\delta - \alpha M_{an}} + \frac{c\, dM_{an}}{dH}. \tag{10}$$

In the case of completely isotropic materials, in which the magnetization has essentially no preferred direction, a phenomenological model of the anhysteretic magnetization, based on modified Langevin function, has been used, giving the equation

$$M_{an}(H) = M_s\left(\coth\left(\frac{H + \alpha M}{a}\right) - \frac{a}{H + \alpha M}\right). \tag{11}$$

Since $M = 0$ at the origin, this leads to the following expression for χ'_{in} on substituting (11) into (10):

$$\chi'_{in} = \frac{(1-c)\left[\coth\left(\frac{H}{a}\right) - \frac{a}{H}\right]}{k\delta - \alpha\left[\coth\left(\frac{H}{a}\right) - \frac{a}{H}\right]} - \frac{c}{a}\left[\operatorname{cosech}^2\left(\frac{H}{a}\right) + \frac{a^2}{H^2}\right] \tag{12}$$

and taking the limit as $H \to 0$ of $\coth(H/a) - (a/H)$,

$$\lim_{H\to 0}\left[\coth\left(\frac{H}{a}\right) - \left(\frac{a}{H}\right)\right] = \lim_{H\to 0}\left\{\frac{a}{H} + \frac{H}{3a} + \cdots - \frac{a}{H}\right\} \tag{13}$$

$$= \lim_{H\to 0}\frac{H}{3a} \tag{14}$$

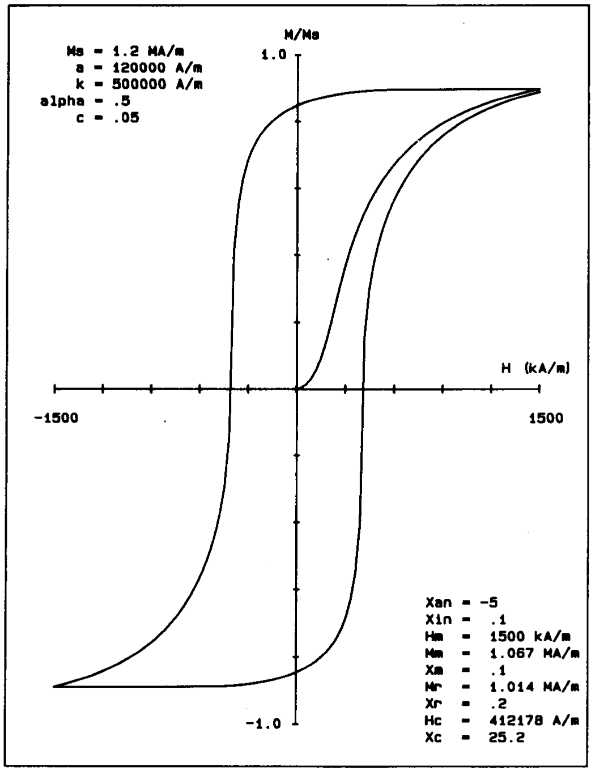

Fig. 4. Theoretical hysteresis loops obtained from solution of the model equations with $M_s = 1.2 \times 10^6$ A · m^{-1}, $a = 120 \times 10^3$ A · m^{-1}, $k = 500 \times 10^3$ A · m^{-1}, $\alpha = 0.5$, $c = 0.05$.

so that

$$\chi'_{\text{in}} = \lim_{H \to 0} \frac{dM}{dH} \tag{15}$$

$$= 0 + \frac{c\,dM_{\text{an}}}{dH}. \tag{16}$$

And since $M = 0$ at the origin of the magnetization curve,

$$\chi'_{\text{in}} = \frac{cM_s}{3a}. \tag{17}$$

This then gives

$$c = \frac{3a\chi'_{\text{in}}}{M_s} \tag{18}$$

which is a direct relationship between c and the initial susceptibility.

Relationship Between a and α

The anhysteretic susceptibility itself gives a relationship between the model parameters a and α. This relationship, of course, depends on the form of the function chosen to model the anhysteretic magnetization curve. The modified Langevin function has been used successfully to model the anhysteretic magnetization, although it should be remembered that this choice of M_{an} is very specific, and that other functions for M_{an} exist for particular circumstances.

From the anhysteretic function given in (11), it is easily shown that the anhysteretic susceptibility at the origin is given by

$$\chi'_{\text{an}} = \lim_{H, M \to 0} \left\{ \frac{d}{dH} (M_{\text{an}}(H) \right\} = \frac{M_s}{3a - \alpha M_s}, \tag{19}$$

and so

$$a = \frac{M_s}{3} \left(\frac{1}{\chi'_{\text{an}}} + \alpha \right). \tag{20}$$

This equation can then be used as a constraint on the model parameters a and α, although a further condition is needed to determine the values of these parameters.

Determination of the Parameter k which Determines the Hysteresis Loss

The coercivity is determined by the amount of pinning, and hence by the parameter k. For very soft magnetic materials, it is found that $k = H_c$, provided k is defined in units of A · m^{-1} as given above. For this reason, the definition of the pinning parameter in units of A · m^{-1} is preferred since the pinning force acts like a field opposing the prevailing magnetic field H. The general relationship between k and H_c can be expressed most simply if the differential susceptibility at the coercive point χ'_{Hc} is known.

Again, we return to (9), and now consider the situation at the coercive point. Let $\chi'_{Hc} = \chi'_{\max}$ denote the differential susceptibility at the coercive point, which in the model is always the maximum value of differential susceptibility observed around the hysteresis loop.

$$\chi'_{\max} = \frac{1}{k\delta - \alpha(M_{\text{an}}(H_c) - M_{\text{irr}})} (M_{\text{an}}(H_c) - M_{\text{irr}}) + c \left(\frac{dM_{\text{an}}(H_c)}{dH} - \frac{dM_{\text{irr}}}{dH} \right) \tag{21}$$

at the position coercive point $\delta - 1$, $H = H_c$, $M = 0$, and rearranging the equation in terms of k leads to

$$k = \frac{1}{\chi'_{\max} - c \left(\frac{dM_{\text{an}}}{dH} (H_c) - \frac{dM_{\text{irr}}}{dH} \right)} (M_{\text{an}}(H_c) - M_{\text{irr}}) + \alpha(M_{\text{an}}(H_c) - M_{\text{irr}}). \tag{22}$$

Explicit equations for M_{irr} and dM_{irr}/dH at the coercive point can be obtained in terms of $M_{\text{an}}(H_c)$, $\chi'_{\max}$, and $dM_{\text{an}}(H_c)/dH$ since it has already been given [3] that

$$M = M_{\text{rev}} + M_{\text{irr}}, \tag{23}$$

and since $M_{\text{rev}} = c(M_{\text{an}} - M_{\text{irr}})$, it follows that

$$M = cM_{\text{an}} + (1 - c)M_{\text{irr}} \tag{24}$$

and rearranging gives

$$M_{irr} = \frac{1}{1-c}(M - cM_{an}). \tag{25}$$

Since $M = 0$ at the coercive point, (25) yields

$$M_{irr} = -\left(\frac{c}{1-c}\right) M_{an}(H_c), \tag{26}$$

while differentiating (25) with respect to H and considering the values at the coercive point gives

$$\frac{dM_{irr}(H_c)}{dH} = \left(\frac{1}{1-c}\right)\chi'_{max} - \left(\frac{c}{1-c}\right)\frac{dM_{an}(H_c)}{dH}. \tag{27}$$

Substituting these expressions into (22) gives the following equation for k:

$$k = \frac{1}{\left(\frac{1}{1-c}\right)\chi'_{max} - \left(\frac{c}{1-c}\right)\frac{dM_{an}(H_c)}{dH}} \cdot \left(\frac{1}{1-c}\right) M_{an}(H_c) + \left(\frac{\alpha}{1-c}\right) M_{an}(H_c), \tag{28}$$

and consequently,

$$k = \frac{M_{an}(H_c)}{1-c} \cdot \left\{\alpha + \frac{1}{\left(\frac{1}{1-c}\right)\chi'_{max} - \left(\frac{c}{1-c}\right)\frac{dM_{an}(H_c)}{dH}}\right\} \tag{29}$$

which can be used to calculate k provided all of the other parameters are known.

Determination of a and α

The remanence point M_r is dependent on α and other parameters. If the other parameters a, k, and c are known, the remanence can be used to calculate α. However, in this case, it has not been possible to obtain an explicit expression for α.

Using the remanence M_r and the differential susceptibility at remanence χ'_r, the parameter a can be determined if the other parameters are already known. Starting from (9), with $\delta = -1$, $H = 0$, and $M = M_r$,

$$\chi'_r = \frac{1}{-k - \alpha(M_{an}(M_r) - M_{irr})}(M_{an}(M_r) - M_{irr}) + c\left(\frac{dM_{an}(M_r)}{dH} - \frac{dM_{irr}}{dH}\right) \tag{30}$$

and since $M_r = M_{rev} + M_{irr}$ and $M_{rev} = c(M_{an} - M_{irr})$, it can be shown that, at remanence,

$$M_{irr} = \frac{M_r - cM_{an}(M_r)}{(1-c)} \tag{31}$$

and

$$\frac{dM_{irr}}{dH} = \left(\frac{1}{1-c}\right)\frac{dM_r}{dH} - \left(\frac{c}{1-c}\right)\frac{dM_{an}(M_r)}{dH}. \tag{32}$$

Substituting these results back into (30) gives

$$\chi'_r = \frac{M_{an}(M_r) - M_r}{-(1-c)k - \alpha(M_{an}(M_r) - M_r)} + \left(\frac{c}{1-c}\right)\left(\frac{dM_{an}(M_r)}{dH} - \frac{dM_r}{dH}\right) \tag{33}$$

and so

$$\left(\frac{1}{1-c}\right)\chi'_r = \frac{M_{an}(M_r) - M_r}{-(1-c)k - \alpha(M_{an}(M_r) - M_r)} + \left(\frac{c}{1-c}\right)\frac{dM_{an}(M_r)}{dH}, \tag{34}$$

and rearranging this equation leads to

$$k(1-c) = \left[\alpha + \frac{1}{\left(\frac{\chi'_r}{1-c}\right) - \left(\frac{c}{1-c}\right)\frac{dM_{an}(M_r)}{dH}}\right] \cdot (M_r - M_{an}(M_r)). \tag{35}$$

This equation can then be used to give an explicit expression for M_r, which is

$$M_r = M_{an}(M_r) + \frac{k}{\left(\frac{\alpha}{1-c}\right) + \frac{1}{\chi'_r - c\frac{dM_{an}(M_r)}{dH}}}. \tag{36}$$

Relationship Between the Hysteresis Parameters at the Loop Tip

Finally, in calculating α and a, it has been found useful to include some redundancy by incorporating the coordinates of the loop tip M_m, H_m and the slope of the initial magnetization curve at the loop tip χ'_m.

We start again from (9) and consider the differential susceptibility along the initial magnetization curve at the loop tip with $\delta = 1$. If the loop tip is sufficiently close to saturation, then the differential susceptibility of the initial magnetization curve at the loop tip will approach the differential susceptibility of the anhysteretic $dM/dH \simeq dM_{an}(H_m)/dH$. This can be used as an approximation to obtain an equation relating the hysteresis parameters. Using the general result $M_{irr} = (M - cM_{an})/(1-c)$, it is easily seen that the above approximation also implies that $dM_{irr}/dH = dM/dH = dM_{an}(H_c)/dH$. In addition, $M_{irr} \approx M_m$ under these conditions.

Replacing M_{irr} with M_m leads to

$$\chi'_m = \frac{}{k - \alpha(M_{an}(H_m) - M_m)}(M_{an}(H_m) - M_m) + c\left(\frac{dM_{an}(H_m)}{dH} - \frac{dM_{irr}}{dH}(H_m)\right). \tag{37}$$

These approximations also allow the second term on the right-hand side of (37) to be eliminated:

$$\chi'_m = \frac{1}{k - \alpha(M_{an}(H_m) - M_m)} (M_{an}(H_m) - M_m), \quad (38)$$

and rearranging this leads to

$$(1 + \alpha\chi'_m)M_m = M_{an}(H_m)(1 + \alpha\chi'_m) - k\chi'_m, \quad (39)$$

and hence,

$$M_m = M_{an}(H_m) - \frac{(1-c)k\chi'_m}{\alpha\chi'_m + 1}. \quad (40)$$

In principle, the incorporation of this equation in the parameter calculation algorithm is not entirely necessary, but it has been found that numerical solutions show faster convergence when this condition is included, and therefore it is a useful practical addition to the previous equations for determining the hysteresis parameters.

Procedure for Calculating Parameters

Since some of the equations needed for determining the parameters can only be expressed implicitly in terms of these and other parameters, a numerical method has been devised for calculating the values by using successive iteration. The reversible coefficient c is obtained directly from the initial slope of the normal magnetization curve using (17). The values of a, α, and k are then obtained by using (29), (36), and (40) successively in an iterative procedure. A seed value of α is used, and from (20), a first estimate of a is found. Then k is calculated from (29). Using the current values of k and a, α is then calculated from (36), and then using the current values of α and k, a is calculated from (40). The procedure for calculating k, α, and a is then repeated.

Sample Calculation of the Hysteresis Parameters

Two model hysteresis loops were calculated using the values of the parameters shown in Table I. From these curves, the values of the various "fixed reference points" were obtained as shown in Table II. These were then used as input data for the parameter calculation program. By using a theoretical curve in this way, the correct values of the hysteresis parameters were known in advance, and the precision of the parameter calculation program could be found from inversion.

The values of the parameters calculated from the inversion algorithm using the results obtained in Figs. 1 and 2 are shown in Table III. From these, it can be seen that the errors encountered in the inversion process in a, k, α, and c are 1.5–3.9%, 2.0–3.7%, 8.0–13.0%, and 2.0–4.0%, respectively. It is felt that further improvements in the algorithm may be possible, such as a least squares fitting procedure over the entire loop; however, most of the errors encountered are now due to the precision with which data can be obtained from the experimental hysteresis loops rather than in the algorithm since the model parameters can be rather sensitive to small changes in the measured magnetic properties.

TABLE I
Hysteresis Parameters Used to Generate the Hysteresis Curves Shown in Figs. 1 and 2, Respectively

	A	B
M_s (A · m^{-1})	1.7×10^6	1.7×10^6
a (A · m^{-1})	1000	1000
k (A · m^{-1})	500	2000
α	1.0×10^{-3}	1.0×10^{-3}
c	0.1	0.1

TABLE II
Magnetic Properties Including Various Susceptibilities, Coercivity, and Remanence Obtained from the Hysteresis Curves in Figs. 1 and 2, Respectively

	A	B
χ'_{an}	1307	1307
χ'_{in}	57	57
H_m (kA · m^{-1})	10	10
M_m (kA · m^{-1})	1546	1507
χ'_m	14.3	25.1
M_r (kA · m^{-1})	503	978
$\chi'M_r$	852	337
H_c (A · m^{-1})	467	1644
$\chi'H_c$	1208	745

TABLE III
Hysteresis Parameters Obtained by the Inversion Algorithm from the Data Given in Table II. These Can Be Compared with the Original Generating Data in Table I

	A	B
M_s (A · m^{-1})	1.7×10^6	1.7×10^6
a (A · m^{-1})	1015	1039
k (A · m^{-1})	490	1927
α	1.08×10^{-3}	1.13×10^{-3}
c	0.102	0.104

Modeling of Experimental Hysteresis Loops

This section discusses the modeling of actual measured hysteresis loops using the theoretical equations. The examples are of specimens of 0.2, 0.4, 0.6, 0.8, and 1.0 wt% carbon steel, the magnetization curves of which are shown in Figs. 5–9. From the magnetization curves, the various "fixed reference points" were obtained and the hysteresis parameters were calculated using the inversion algorithm. The theoretical curves are also shown in Figs. 5–9, and these show excellent agreement with the experimental results. For example, for the 1 wt% C steel, the measured coercivity was 1509 A · m^{-1} (compared with 1538 A · m^{-1} using the model), the remanence was 0.72 $\times 10^6$ A · m^{-1} (compared with 0.68 $\times 10^6$ A · m^{-1}), and the initial differential susceptibility was 45 (compared

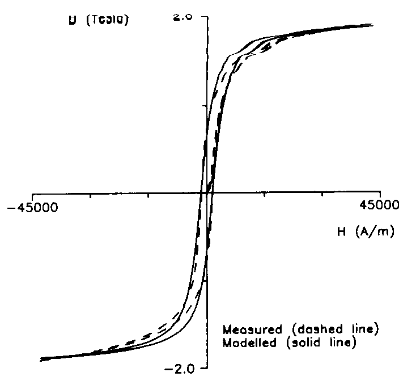

Fig. 5. Comparison of measured and modeled hysteresis curves of a specimen of 1.0 wt% C carbon steel.

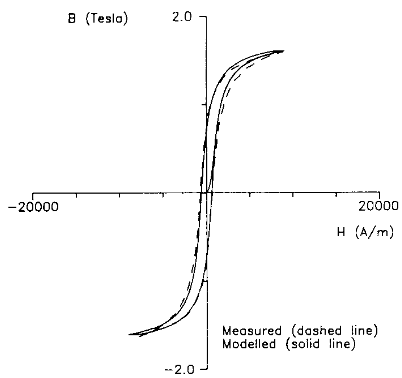

Fig. 6. Comparison of measured and modeled hysteresis curves for a specimen of 0.8 wt% C steel.

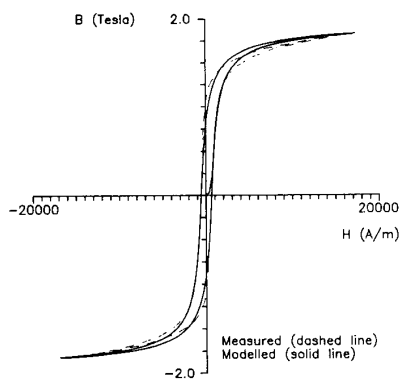

Fig. 7. Comparison of measured and modeled hysteresis curves for a specimen of 0.6 wt% C steel.

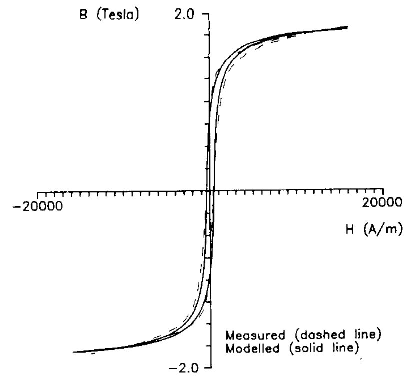

Fig. 8. Comparison of measured and modeled hysteresis curves for a specimen of 0.4 wt% C steel.

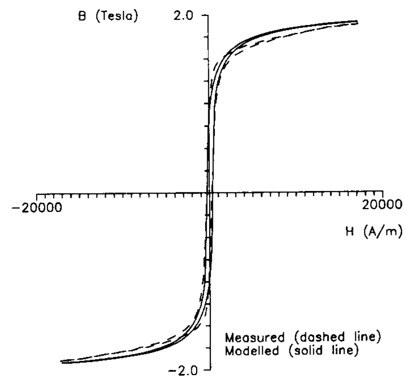

Fig. 9. Comparison of measured and modeled hysteresis curves for a specimen of 0.2 wt% C steel.

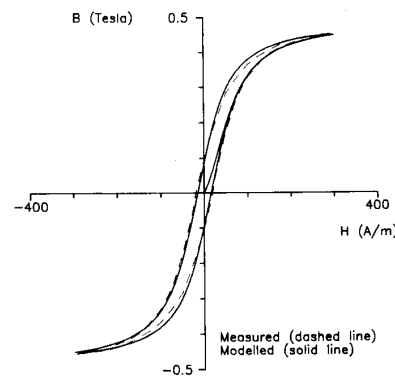

Fig. 10. Comparison of measured and modeled hysteresis curves for a specimen of 3C8 manganese–zinc ferrite.

with 41), which is a dimensionless quantity. A comparison of the observed and modeled results for this specimen is given in Tables IV and V.

Summary of Results

The hysteresis loops of a wide range of magnetic materials can be modeled using the equations given above. The hysteresis parameters were calculated from the various intercepts and slopes taken from experimental hysteresis loops. At present, it is still necessary to obtain these parameters from a curve-fitting procedure, even though a physical description of the effects of these various parameters has been given previously. It is desirable, however, that these parameters be obtained, where pos-

TABLE IV
MEASURED MAGNETIC PROPERTIES OF MATERIALS SHOWN IN FIGS. 5–10

		Fe 1.0 wt% C	Fe 0.8 wt% C	Fe 0.6 wt% C	Fe 0.4 wt% C	Fe 0.2 wt% C	3C8 Mn–Zn Ferrite
B_s	Saturation induction (tesla)	1.9	2.0	2.0	2.0	2.0	0.5
μ'_{an}	Initial anhysteretic relative permeability	1000	1343	2000	2700	5000	6500
μ'_{in}	Initial relative permeability	45	142	75	104	100	2700
H_m	Field at loop tip (A/m)	43 600	8883	17 000	16 000	17 200	240
B_m	Induction at loop tip (tesla)	1.88	1.62	1.85	1.83	1.94	0.46
μ_m	Relative differential permeability at loop tip	6	5	7	5	5	190
B_r	Remanence (tesla)	0.72	0.81	1.1	0.91	0.88	0.10
μ_r	Relative differential permeability at remanence	213	508	650	1000	1200	4250
H_c	Coercivity (A/m)	1509	693	620	400	315	16
μ'_c	Relative differential permeability at coercive point	750	1034	1520	1200	1520	6250

TABLE V
MODEL HYSTERESIS PARAMETERS M_s, a, k, α, AND c AS OBTAINED FROM THE MEASURED HYSTERESIS CURVES SHOWN IN FIGS. 5–10

	Fe 1.0 wt% C	Fe 0.8 wt% C	Fe 0.6 wt% C	Fe 0.4 wt% C	Fe 0.2 wt% C	3C8 Mn–Zn Ferrite
M_s	1.5×10^6	1.6×10^6	1.6×10^6	1.6×10^6	1.6×10^6	0.4×10^6
a	1800	1000	972	1010	1085	27
k	1800	700	672	455	320	30
α	1.4×10^{-3}	1.4×10^{-3}	1.4×10^{-3}	1.8×10^{-3}	2×10^{-3}	5×10^{-5}
c	0.14	0.22	0.14	0.21	0.3	0.55
B_s	1.9	2.0	2.0	2.0	2.0	0.5
μ'_{an}	461	1450	1987	4203	22 165	6512
μ'_{in}	41	110	78	112	155	2686
H_m	40 000	9000	17 000	16 000	17 200	240
B_m	1.87	1.6	1.82	1.81	1.91	0.44
P_m	2.4	14.9	5.4	5.7	5.4	200
B_r	0.68	0.71	0.85	0.86	0.91	0.10
μ_r	278	586	580	648	706.4	5064
H_c	1538	617	624	441	337	15
μ_c	389	1206	1633	3236	5571	5718

The model parameters were first obtained from the parameter calculation algorithm by using the measured properties at the origin, loop tip, remanence, and coercivity. This gave a first approximation based only on four points on the curve. The parameters were then optimized manually to obtain a better fit over the entire range of the measured hysteresis loop.

Also shown in the table are the modeled magnetic properties (μ'_{an}, μ'_{in}, etc.) obtained by calculating the hysteresis loop using the given model parameters (M_s, a, k, α, and c).

sible, from first principles. In particular, the parameter a, which can be described as a form factor for the anhysteretic curve, presents a problem since, although it is clearly temperature dependent, it does not seem to simply represent the Boltzmann energy $k_B T$ unless a regular array of pseudodomains (domains of equal magnetic moment) is assumed. It is affected by anisotropy and texture, resulting in different anhysteretic magnetization curves along different directions in a textured material.

Although this goal of providing a more fundamental interpretation of the hysteresis parameters is being pursued, it must be remembered that the scaling up of microscopic theories (e.g., a single domain wall/defect interaction) to account for macroscopic properties (e.g., magnetization curves) is a formidable problem which is fraught with difficulties. Furthermore, it is unlikely that a parameter such as k will be interpretable other than as a statistical averaged of all the domain wall pinning mechanisms occurring in the material.

CONCLUSIONS AND FUTURE WORK

The objective of this paper is to show how the hysteresis parameters a, α, k, and c can be determined from experimental hysteresis measurements, and then used to model the hysteresis curves using the theory of hysteresis. This represents a new development of the modeling of ferromagnetic hysteresis which makes it possible for the first time to calculate the generating parameters for this model from a set of experimental data. It has been shown that the method described is capable of determining the values of these parameters to within an error of a few percent. A comparison of measured and modeled hysteresis loops has also been given which shows excellent agreement between the modeled and measured curves.

In the future, two further contributions to hysteresis need to be incorporated into the model. These are magnetocrystalline anisotropy and texture. Magnetocrystalline anisotropy will contribute to additional coercivity which could be described by anisotropic rotation models such as that of Stoner and Wohlfarth [8]. It may therefore be anticipated that the magnetocrystalline anisotropy will emerge as an independent contribution to the parameter k in the present model. Texture (preferred orientation) in the presence of magnetocrystalline anisotropy will lead to preferred axes of magnetization within the bulk specimen. This should emerge as changes in the anhysteretic magnetization curve $M_{an}(H)$, which will then assume an angular dependence, as described by Furlani and Baker [5]. The net result will be differences in the differential susceptibility χ' of the model along particular directions of the specimen, as observed in practice.

Finally, it is felt that although the two differential equations of hysteresis (6) and (8) represent the underlying mechanism of hysteresis, the choice of a function for the anhysteretic magnetization M_{an} must depend on the details of the particular material chosen (e.g., whether texture is present). So far, a phenomenological model using the modified Langevin equation (18) has been used since this has worked satisfactorily in a large number of cases. It is, however, applicable only to isotropic media, but gives good results for soft magnetic materials such as iron and steel. It should not be thought of as totally general, and consequently, an appropriate function for M_{an} should be chosen for each particular material.

References

[1] D. C. Jiles and D. L. Atherton, *J. Appl. Phys.*, vol. 55, p. 2115, 1984.
[2] —, *J. Phys. D*, vol. 17, p. 1265, 1984.
[3] —, *J. Magnetism Magn. Mater.*, vol. 61, p. 48, 1986.
[4] J. A. Szpunar and B. Szpunar, *J. Appl. Phys.*, vol. 57, p. 4232, 1985.
[5] E. P. Furlani and A. G. Baker, *J. Appl. Phys.*, vol. 59, p. 3815, 1986.
[6] P. Garikepati, T. T. Chang, and D. C. Jiles, *IEEE Trans. Magn.*, vol. 24, p. 2922, 1988.
[7] D. C. Jiles and J. B. Thoelke, *IEEE Trans. Magn.*, vol. 25, p. 3928, 1989.
[8] E. C. Stoner and E. P. Wohlfarth, *Phil. Trans. Roy. Soc. (London)*, vol. A240, p. 599, 1948.

David C. Jiles (M'83–SM'89) received the Ph.D. degree in applied physics from the University of Hull, Hull, England, in 1979, and studied at Victoria University, New Zealand, and Queen's University, Canada.

He joined the Ames Laboratory, Iowa State University, in 1984 and the Center for NDE in 1986. He is currently a Senior Physicist with Iowa State University's Institute for Physical Research and Technology and Professor of Materials Science and Engineering. He is the author of over 100 scientific and technical papers, and the author of the book, *Introduction to Magnetism and Magnetic Materials* (1990).

Dr. Jiles is a Fellow of the Institute of Physics and a member of the American Society for Materials, the Metallurgical Society, and the American Society for Nondestructive Testing. He is a Registered Professional Engineer, serves as a consultant for several companies both in North America and Europe, and was awarded a higher doctorate in physics in 1990 by the University of Birmingham for his work on the magnetic and electronic properties of metals.

J. B. Thoelke, biography not available at the time of publication.

M. K. Devine, received the B.S. degree in metallurgical engineering from the Illinois Institute of Technology in 1989. He is presently working towards the M.S. degree in material science and engineering at Iowa State University, Ames.